Polycystin 1 is required for the structural integrity of blood vessels

Keetae Kim[†], Iain Drummond[†], Oxana Ibraghimov-Beskrovnaya[‡], Katherine Klinger[‡], and M. Amin Arnaout[†§]

[†]Renal Unit, Massachusetts General Hospital, Harvard Medical School, Charlestown, MA 02129; and [‡]Genzyme Corp., Framingham, MA 01701

Communicated by Patricia K. Donahoe, Massachusetts General Hospital, Boston, MA, December 16, 1999 (received for review November 1, 1999)

Autosomal dominant polycystic kidney disease (ADPKD), often caused by mutations in the PKD1 gene, is associated with life-threatening vascular abnormalities that are commonly attributed to the frequent occurrence of hypertension. A previously reported targeted mutation of the mouse homologue of PKD1 was not associated with vascular fragility, leading to the suggestion that the vascular lesion may be of a secondary nature. Here we demonstrate a primary role of PKD1 mutations in vascular fragility. Mouse embryos homozygous for the mutant allele (*Pkd1*^{L}) exhibit s.c. edema, vascular leaks, and rupture of blood vessels, culminating in embryonic lethality at embryonic day 15.5. Kidney and pancreatic ductal cysts are present. The *Pkd1*-encoded protein, mouse polycystin 1, was detected in normal endothelium and the surrounding vascular smooth muscle cells. These data reveal a requisite role for polycystin 1 in maintaining the structural integrity of the vasculature as well as epithelium and suggest that the nature of the PKD1 mutation contributes to the phenotypic variance in ADPKD.

homologous recombination | angiogenesis | tight junctions | polycystic kidney disease

Autosomal dominant polycystic kidney disease (ADPKD) is the most common monogenic disease in humans, with a frequency ranging from 1:400 to 1:1,000 persons (1). The cardinal feature of ADPKD is the formation of cysts in both kidneys (2), which originate from fewer than 1% of all nephrons (3), and lead over time to progressive destruction of normal renal tissue and end-stage kidney failure in more than 50% of patients. There is also a high prevalence of extrarenal manifestations in ADPKD. These consist of cyst formation in other ductal organs and vascular abnormalities including aneurysms in the cerebral and coronary blood vessels (4). Intracranial aneurysms are observed in approximately 10% of asymptomatic adults with ADPKD (5, 6), and the aneurysms' sudden rupture is responsible for death in up to 20% of the cases (7). Clustering of intracranial aneurysms has been described in several ADPKD families, with the incidence rising to 25% in the asymptomatic patients (5, 6). Furthermore, retrospective analysis of renal tissue from patients with ADPKD reveals sclerotic vascular changes present early in the course of the disease, which may contribute to the progressive loss of renal function (8). The vascular abnormalities seen in ADPKD commonly are attributed to hypertension that frequently complicates the course of ADPKD.

In 85–95% of the cases of ADPKD, the disease is caused by heterogeneous mutations in the PKD1 gene. PKD1 encodes polycystin 1, an 11-pass membrane protein with a large extracellular region composed of a unique compilation of potential adhesion and protein–protein interaction domains (9, 10). In ≈5–15% of cases, a second gene (*PKD2*) is responsible, and the disease is generally milder. PKD2 encodes polycystin 2, a six-pass membrane protein with homology to voltage-activated calcium channels (11, 12). In a small number of families, a third yet-to-be-characterized gene has been implicated (13). Polycystins are expressed in epithelia (14–17). Polycystin 1 also has been detected in endothelial and vascular smooth muscle cells (18, 19). Polycystin 1 has been found at cell–cell junctions in endothelial (19) and epithelial (20) cell monolayers. Mouse models with targeted mutations in PKD1 (21) and PKD2 (22) develop renal, pancreatic, and liver cysts, but not the vascular fragility seen in humans. This finding implied that the vascular abnormalities seen in ADPKD may be secondary in nature.

In this paper, we show that mice homozygous for a targeted mutation in the mouse homologue of PKD1 die *in utero* between 14.5 and 15.5 days postcoitum [embryonic day (E) 14.5–15.5], most likely the result of massive hemorrhage. At earlier time points (E12.5–13.5), s.c. edema and focal vascular leaks and hemorrhage are present. Focal hemorrhage often is seen in tissues undergoing angiogenesis. Renal and pancreatic cysts are seen beginning at E13.5. Immunostaining revealed that wild-type (WT) as well as mutant polycystin 1 are expressed in epithelium, endothelium, and vascular smooth muscle. Taken together, these findings indicate that phenotypic variability in ADPKD is caused in part by the nature of the PKD1 mutation, and that polycystin 1 is essential for maintaining the integrity of blood vessels, in addition to mature epithelium.

Methods

Generation of *Pkd1* Knockout Mice. We isolated a mouse genomic clone containing the mouse PKD1 homologue (*Pkd1*) by screening a library with the human cDNA probe 3A3 (9). The mouse genomic fragment was used to isolate a larger murine (strain 129sv) Bac clone. A 6-kb *Eco*RI–*Xba*I and a 4-kb *Not*I-restricted murine *Pkd1* fragments were generated by PCR, confirmed by sequencing, and cloned on either side of the *neo* gene in the double selection plasmid pPNT (which contains a neomycin phosphotransferase, *neo,* controlled by the phosphoglycerol kinase promoter for positive selection and a herpes simplex virus thymidine kinase, HSVTK, gene for negative selection). The *neo* cassette was placed in the opposite transcriptional orientation to the *Pkd1* gene. In the resulting mutant allele, portions of exons 43 and 45 and all of exon 44 are replaced by the *neo* cassette, and a stop codon was introduced at the end of the remaining segment of exon 43. The J1 line of embryonic stem (ES) cells (23) was grown on subconfluent γ-irradiated embryonic fibroblasts (24) and used for transfections. The linearized recombination vector was electroporated into J1 ES cells. Two independent ES clones (#130 and #282) heterozygous for the mutant allele (*Pkd1*^{L}) were identified through probing *Kpn*I-digested DNA with the 5′ cDNA probe and were injected into blastocysts from C57 black mice. Blastocysts then were placed into pseudopregnant female mice. Chimeric mice were used for breeding with WT C57 black mice. The male chimeras were mated with normal females to

Abbreviations: ADPKD, autosomal dominant polycystic kidney disease; E(*n*), embryonic day; WT, wild type; ES, embryonic stem; TSC2, tuberous sclerosis 2; LRR, leucine-rich repeats.

§To whom reprint requests should be addressed at: Renal Unit, Massachusetts General Hospital, 149 13th Street, Charlestown, MA 02129. E-mail: arnaout@receptor.mgh.harvard.edu.

The publication costs of this article were defrayed in part by page charge payment. This article must therefore be hereby marked "*advertisement*" in accordance with 18 U.S.C. §1734 solely to indicate this fact.

Article published online before print: *Proc. Natl. Acad. Sci. USA*, 10.1073/pnas.040550097. Article and publication date are at www.pnas.org/cgi/doi/10.1073/pnas.040550097

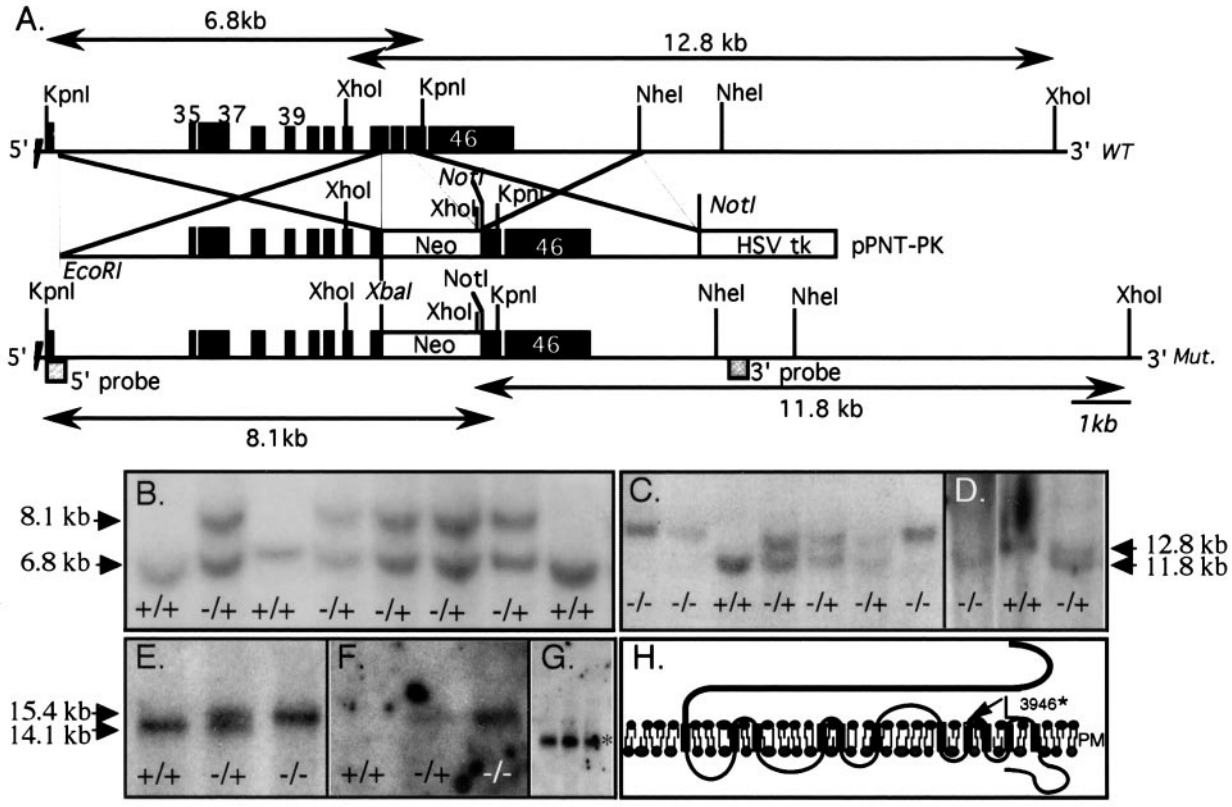

Fig. 1. Targeted disruption of mouse *Pkd1*. (*A*) The genomic segment of WT and recombinant murine *Pkd1*. Exons (black boxes) are numbered. The position of the recombinations, the expected sizes of WT and mutant (Mut.) fragments, and the position of the external 5′ and 3′ probes are indicated. (*B*) Southern blots of genomic DNA extracted from ES clones, *Kpn*I-restricted, and probed with the 5′ external probe. A recombinant mutant fragment (8.1 kb) replaces the normal allele (6.8 kb) in several clones. DNA from clone #282 and #130 is shown in lanes 2 and 6. (*C* and *D*) Germ-line transmission of the mutant allele. Yolk sac DNA obtained from the offspring of F_1 intercrosses was extracted, digested with *Kpn*I or *Xho*I, and probed, respectively, with the 5′ (*C*) or 3′ (TSC2 exon 33, 430 bp, *D*) probes. Fragment size is indicated by arrows. Southern blots of DNA from clone #282 (lanes 1–4 in *C* and 1–3 in *D*) and #130 (lanes 5–7, *C*) F_2 embryos is shown. $+/+$, $+/-$, and $-/-$ indicate WT, $Pkd1^{+/L}$, and $Pkd1^{L/L}$, respectively. (*E*–*G*) Northern blot analysis. The mutant allele (15.4 kb) is found in $Pkd1^{L/L}$ (lane 3) and $Pkd1^{+/L}$ (lane 2) but not WT animals, who express only the WT mRNA of 14.1 kb (lane 1). The mutant but not the WT allele hybridized with the *neo* probe (*F*). (*G*) The normal-sized mRNA for mouse TSC2 (5.6 kb, ∗) in $Pkd1^{L/L}$ embryos. (*H*) Primary structure of polycystin 1 and the site of the predicted truncation (arrow). Mutant mouse polycystin 1 is expected to terminate after L3946 (equivalent to L3955 in human).

generate heterozygous mice $Pkd1^{+/L}$. WT, $Pkd1^{+/L}$, and $Pkd1^{L/L}$ embryos and mice were identified by Southern blot analysis of *Kpn*I- or *Xho*I-restricted yolk sac and tail DNA, respectively.

***In Vivo* Assessment of Vascular Leak.** E12.5 embryos were maintained in PBS and positioned in an agarose trough for injection. Micropipets filled with dye solution [0.5% lysinated FITC-dextran (70 kDa; Molecular Probes), 0.2% trypan blue in PBS containing 1 mM $CaCl_2$ and 1 mM $MgCl_2$] were introduced into the anterior cardinal vein. A total volume of 1–2 μl of dye solution was injected over a period of 5–10 min. Successful introduction of dye was monitored visually by using trypan blue. All embryos had active circulation at the time of injection as assessed by blood flow in the anterior cardinal vein. Immediately after injection, embryos were fixed in 4% paraformaldehyde/PBS. After dehydration and embedding in glycol methacrylate (JB-4; Polysciences), 4-μm sections were cut on glass knives and mounted in vectashield (Vector Laboratories) for fluorescence microscopy.

Antibody Preparation. Specific anti-human polycystin 1 polyclonal antibodies against three different glutathione *S*-transferase-fusion proteins were produced in rabbits (19). Fusion proteins FP-LRR (leucine-rich repeats) (residues 27–360), FP-BD3 (residues 4097–4302) (19), and FP-L2 (containing part of the receptor for egg jelly-like (REJ) domain of polycystin-1, residues 2714–3074) were generated by using pGEX vectors (Amersham Pharmacia) and purified. The antipeptide antibodies AP-1 and AP-2, directed, respectively, against regions in the REJ and cytoplasmic C-terminal domains of human polycystin 1 have been described (16).

Embryo Tissue Preparation and Immunostaining. Embryos were fixed overnight at 4°C in 4% paraformaldehyde/PBS immediately after harvesting. WT, $Pkd1^{+/L}$, and $Pkd1^{L/L}$ embryos were embedded in paraffin, sectioned into 5-μm thick sections, and stained with hematoxylin and eosin. Sections were mounted in Permount (Fisher) and observed by using a light microscope. For immunostaining, a standard immunoperoxidase protocol (Vectastain ABC kit, Vector Laboratories) was used. Paraffin sections were deparaffinized in xylene, rehydrated in graded ethanol, rinsed in tap water, and treated with trypsin (50 μg/ml in PBS), before a 2-min microwave heating in citrate buffer, pH 6.0 (18). After blocking with 2% goat serum, sections were incubated with the primary antibodies (2 μg/ml) for 1 hr at room temperature, rinsed in PBS, incubated with biotinylated goat anti-rabbit secondary antibodies, rinsed, then incubated with diaminobenzidine as a chromogen, counterstained with hematoxylin and eosin, and examined by light microscopy.

Table 1. Genotype and hemorrhagic phenotype of offspring from *Pkd1*^{L} heterozygote crosses

Stage	*Pkd1*$^{+/+}$	*Pkd1*$^{+/L}$	*Pkd1*$^{L/L}$	ND*	Total
282 line					
E11.5	11	18	7 (0)†	0	36
E12.5	12	21	9 (3)	2	43
E13.5	15	17	12 (7)	1	55
E14.5	17	23	14 (8)	2	56
E15.5	12	19	9 (7)	1	41
E16.5	10	18	0	0	28
E17.5	6	11	0	0	17
Weanling	16	29	0	0	45
130 line					
E11.5	7	14	5 (0)†	0	26
E12.5	10	14	5 (2)	1	30
E13.5	6	15	8 (4)	1	29
E14.5	12	18	7 (3)	2	39
E15.5	8	14	6 (5)	1	29
E16.5	6	10	0	0	16
E17.5	5	9	0	0	14
Weanling	11	24	0	0	35

*ND, genotype not determined.

†The number of hemorrhagic phenotype is indicated in parentheses among homozygous mutants. All homozygous mutants had gross edema at every gestational age examined beyond E13.5.

Results

Mice Homozygous for the *Pkd1*^{L} Allele Die *in Utero*. The targeted strategy for *Pkd1* and genotype analysis of ES clones and mice are summarized in Fig. 1 *A–D*. Of 184 recombinant ES cell clones screened, four were heterozygous for the mutant *Pkd1*^{L} allele by Southern blotting. Two independent clones (#130 and #282) produced ≈80% and 100% chimeric mice, respectively. Chimeras were crossed with WT C57BL/6 mouse strain. Clone #130-F_2 progeny were derived from six females. Genotyping showed 11 WT, 24 *Pkd1*$^{+/L}$, and no *Pkd1*$^{L/L}$ animals. Clone #282-F_2 progeny were derived from seven females, and genotyping revealed 16 WT, 29 *Pkd1*$^{+/L}$, and again no *Pkd1*$^{L/l}$ animals. Most of the phenotypic analyses were performed with the #282-derived mouse line, but identical results also were obtained with the #130-derived line (Table 1). The heterozygous F_1 and F_2 mice, up to 7 months of age, were apparently normal and fertile. The lack of viable *Pkd1*$^{L/L}$ newborns from *Pkd1*$^{+/L}$ crossings, even though the ratio of WT to *Pkd1*$^{+/L}$ offspring was normal, suggests that homozygosity for the *Pkd1*^{L} allele is embryonically lethal. Northern blot of total RNA derived from WT, *Pkd1*$^{+/L}$, and *Pkd1*$^{L/L}$ mice revealed that the mutant transcript (≈15.4 kb) is expressed in heterozygous and homozygous embryos (Fig. 1*E*), as is often the case in ADPKD. Probing the same Northern blot with a cDNA encoding the *neo* gene showed that the probe hybridized to the 15.4-kb species but not to WT, indicating that the mutant mRNA, contains the introduced *neo* construct, which accounts for its slower mobility. The introduced recombination did not affect the integrity of the adjacent tuberous sclerosis 2 (TSC2) gene, defects of which are known to contribute to the severity of cystic disease in humans (9). This is reflected by the normal size and abundance of TSC2 mRNA (Fig. 1*G*).

To determine the time at which lethality occurs, embryos from F_1 intercrosses were examined at different developmental stages. Analysis of F_2 embryos at midgestation showed that until E12.0 there were no gross morphological differences between *Pkd1*$^{L/L}$ and their *Pkd1*$^{+/L}$ littermates (not shown). In contrast, by E12.5, s.c. edema and small hemorrhages were observed in 35% (five of 14) of the *Pkd1*$^{L/L}$ embryos from both lines (Fig. 2, Table 1). By day E15.5, most *Pkd1*$^{L/L}$ embryos had died, exhibiting extensive hemorrhage and diffuse edema (Fig. 2). No viable *Pkd1*$^{L/L}$ embryos were found at E16.5 or later. These findings suggest that a vascular defect in *Pkd1*$^{L/L}$ embryos results in edema formation, leading to frank hemorrhage and lethality by E15.5.

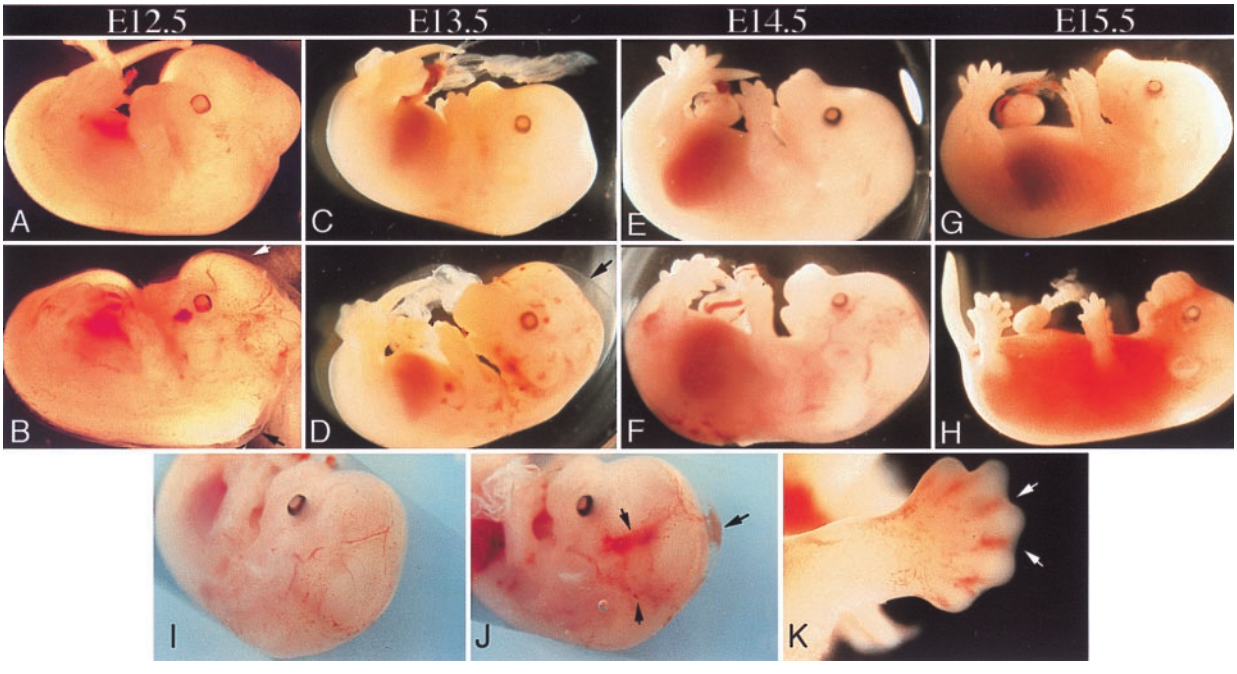

Fig. 2. Gross phenotype of *Pkd*$^{L/L}$ embryos at different stages of development. Whole mounts of *Pkd*$^{L/L}$ (*B*, *D*, *F*, *H*, *J*, and *K*) and age-matched WT embryos (*A*, *C*, *E*, *G*, and *I*) are shown. Localized hemorrhages and s.c. edema (arrows) distributed over the body surface, with punctate and localized hemorrhages seen in the head (*B*, *D*, and *J*) and toes (*H* and *K*) of *Pkd1*$^{L/L}$ (*J*, *H*, and *K*) but not WT (*A*, *C*, *E*, *G*, and *I*) unstained embryos. At E15.5, fatal hemorrhages and edema are seen in *Pkd*$^{L/L}$ embryos (*H*). Staged embryos were dissected in PBS and photographed by using a Leica MZ12 microscope.

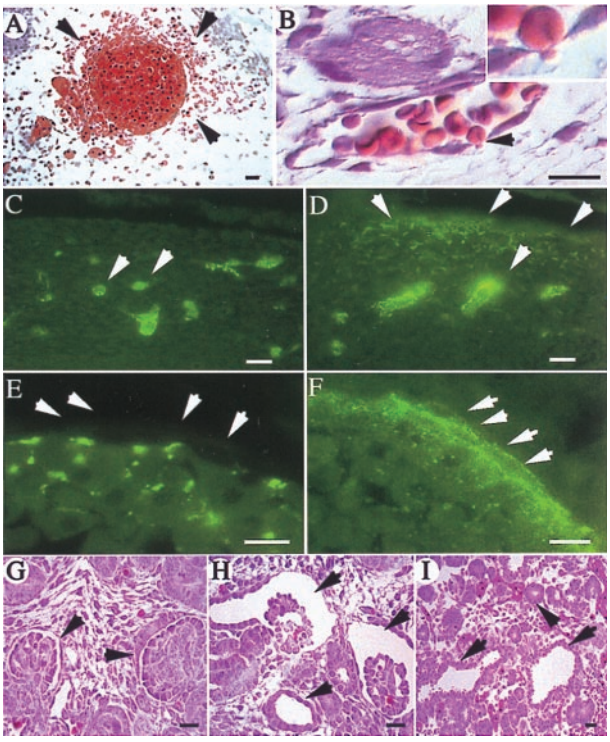

Fig. 3. Histological analysis of tissues from *Pkd1*$^{L/L}$ embryos. (*A*) Hematoxylin and eosin stain showing red blood cells (arrowheads) outside a blood vessel in the neck region at E13.5. (*B*) A skin capillary at E13.5 from a region not showing gross hemorrhage. A red blood cell *(*arrowhead and *Inset)* is seen traversing the endothelial cell lining between two adjacent cells. (*C–F*) Tissue sections revealing the leak of intravascularly injected fluorescent dextran into the extravascular interstitium (*D*, arrows) at distant sites in a E12.5 *Pkd*$^{L/L}$ embryo (*D* and *F*). In the age-matched WT (*C* and *E*), dextran is retained within the vasculature (arrows). No fluorescence is seen on the basolateral side of the lining endothelium in WT embryos (*E*, arrows). In contrast, fluorescent dextran is seen basolaterally (*F*, arrows) and at intercellular junctions in the mutant. (*G–I)* Hematoxylin and eosin stain of a section of a normal developing kidney at E14.5 (*G*), showing two normal glomeruli (arrowheads). An age-matched *Pkd*$^{L/L}$ kidney (*H*) shows two large glomerular cysts (arrows), and a tubular cyst (arrowhead). (*I*) A section of a pancreas from this *Pkd*$^{L/L}$ embryo shows two tubular cysts (arrows) adjacent to normal-sized ducts (arrowhead). Sections shown in *A*, *B*, *G*, *H*, and *I* are 5 μm thick, and those in *C–F* are 4 μm thick. (Scale bars = 10 μm, except in *E* and *F* where the scale bar = 5 μm.)

Vascular Leak and Hemorrhage in *Pkd1*$^{L/L}$ Embryos. Histological analysis of tissue sections from *Pkd1*$^{L/L}$ at E13.5 showed localized areas of hemorrhage in multiple regions of the embryo such as the neck (Fig. 3*A*), skin (Fig. 3*B*), and brain (see below). In skin tissue with no frank hemorrhage, red blood cells were seen traversing apparently intact vascular endothelium at cell–cell junctions (Fig. 3*B*). Microinjection of fluorescent dextran (molecular mass 70 kDa) into the anterior cardinal vein of live WT and mutant E13.5 embryos revealed that while the tracer remained in the intravascular compartment in WT animals, it extravasated to the basolateral regions of endothelium and into the extravascular interstitium at distant sites (Fig. 3 *C–F*). The cell–cell junctions at apparently normal sites in *Pkd1*$^{L/L}$ embryos were well formed as judged by electron microscopy (data not shown). There were no gross histologic abnormalities in the heart or lungs.

Cyst Formation in *Pkd1*$^{L/L}$ Mouse Embryos. Renal and pancreatic cysts were observed at E14.5 in *Pkd1*$^{L/L}$ embryos (Fig. 3 *H* and *I*). In the kidneys, they first appeared as multifocal microscopic dilations of well-developed renal glomerular and tubular structures. Earlier stages of nephrogenesis (mesenchymal condensation, epithelialization) were unaffected. The lesion in the pancreas was again focal and manifested as dilation of pancreatic ducts; Acini appeared normal. No cysts were observed in the liver, as also was observed by Lu *et al.* (21) in another mouse model of ADPKD caused by a different mutation in *Pkd1*. Liver cysts were detected in PKD2 knockout mice ranging in age from 1 to 25 weeks (22). The lack of liver cysts in the two *Pkd1* models suggests that liver cyst formation may require a longer time or is influenced by the nature of the mutation.

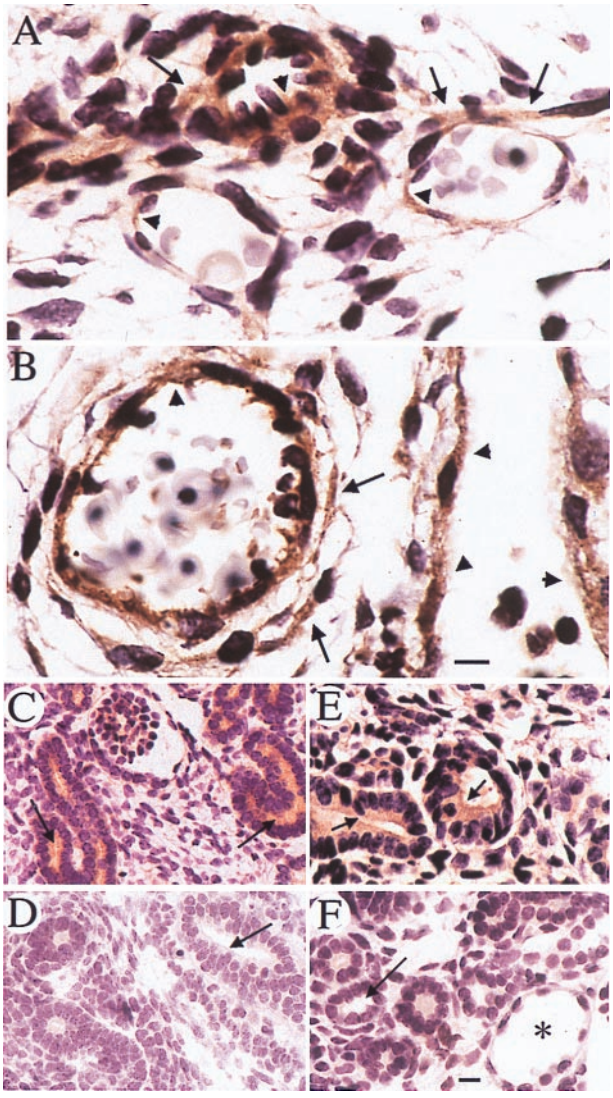

Fig. 4. Expression of polycystin 1 in WT and *Pkd1*$^{L/L}$ *E14.5* mouse embryos. Polycystin 1 is detected in endothelial cells (arrowheads in *A* and *B*) as well as in vascular smooth muscle cells (arrows in *A* and *B*) by using the anti-LRR antibody. Polycystin 1 expression (horseradish peroxidase reaction product) is similar in small vessels in the region of the hind limb in WT (*A*) and *Pkd1*$^{L/L}$ mutant (*B*) embryos. In fetal kidneys, polycystin 1 expression is observed mainly on the apical (arrows in *C* and *E*) surfaces of WT and *Pkd1*$^{L/L}$ renal tubules. No staining of renal tubules (arrows) from either WT or *Pkd1*$^{L/L}$ embryos is observed in the presence of a 20-fold excess of the LRR fusion protein (*D* and *F,* respectively). * in *F* points to a tubular cyst. (Scale bars = 10 μm.)

WT and Mutant Polycystin 1 Are Expressed in Endothelium and Smooth Muscle. As shown in Fig. 4, immunostaining with anti-LRR antibody showed that polycystin 1 was expressed in capillary and small vessel endothelium in both WT and mutant at E14.5 embryos (Fig. 4 *A* and *B*). It was not detected in endothelium of

major vessels in WT and mutant animals (data not shown). Polycystin 1 was detected in smooth muscle of blood vessels (Fig. 4 *A* and *B*), skeletal muscle, and the gut (not shown). Very similar patterns of staining of polycystin 1 were observed by using the anti-receptor for egg jelly-like domain antibody (data not shown). WT and mutant polycystin 1 also were expressed in developing nephrons (Fig. 4 *C* and *E*), as we previously reported (16), and in pancreatic ductal epithelium by using anti-LRR (data not shown). The antibody staining pattern was abolished in the presence of a 20-fold molar excess of the immunogen (Fig. 4 *D* and *F*). The anticytoplasmic tail antibodies BD3 and AP2 and AP1 did not react reproducibly with WT mouse embryos (not shown).

Discussion

The major finding in this paper is that a targeted mutation in *Pkd1* produces embryonic lethality at E15.5 in homozygous mice, secondary to vascular leaks and massive hemorrhage. Renal and pancreatic cysts are seen, as has been previously noted in mice homozygous for a different allele, *Pkd1Δ34* (21). The vascular lesion reflects a crucial and direct role of polycystin 1 in the vasculature, as the WT protein was readily detected in endothelium and the underlying vascular smooth muscle cells. The major axial vessels such as the aorta, formed by vasculogenesis (25), appear normal in the $Pkd1^{L/L}$ embryos. Involvement of blood vessels from brain, skin, and limb buds in the $Pkd1^{L/L}$ embryos, which develop by angiogenesis (26), suggest that polycystin 1 is required for the maturation and/or stability of angiogenically derived blood vessels, in addition to its role in maintaining the structural integrity of ductal epithelium.

In a previous study, Lu *et al.* (21) found that mice homozygous for a frameshift mutation in *Pkd1*, *Pkd1Δ34,* display massive renal and pancreatic cysts, with secondary pulmonary hypoplasia and perinatal mortality. Edema also has been described in these mice, but no vascular lesions were reported. It may appear counterintuitive that the L3946* mutant polycystin 1 (Fig. 1*H*), which is 478 aa longer than the one encoded by the frameshift *Pkd1Δ34* mutant (21), should produce a more severe phenotype as judged by embryonic lethality at E15.5 and display a major vascular phenotype. The fact that embryos generated from two independent recombinant ES cell lines exhibited the same phenotype argues against an aberrant insertion of the mutant gene and/or a functionally relevant recombination event. The presence of a normal-sized TSC2 mRNA argues against an unintended recombination in the 3′ region of *Pkd1* impairing the TSC2 gene. Hybridization of the mutant 15.5-kb mRNA with the *neo* probe confirms that a mutant form of *Pkd1* was produced. A genetic background effect is also unlikely, because our chimeric mice were crossed with C57BL/6 mice to produce the $Pkd1^{+/L}$ progeny, as in the case of some of the mutant mice generated by Lu *et al.* (21). The present data therefore suggest that the longer form of mutant polycystin 1 is responsible for the more severe phenotype. There are other precedents where longer forms of a mutant protein can produce a more severe phenotype than shorter or even null versions. CFTR (cystic fibrosis transmembrane conductance regulator) (27) and WT1 (28) are two such examples. The developmental effects of a loss of WT1 for example are in general less severe than point mutations affecting its DNA binding domain (28).

The L3946* mutant contains two intracellular, two extracellular loops, and five transmembrane segments that all are lacking in the mutant encoded by *Pkd1Δ34* allele (21). This region is highly conserved in human, mouse, and fish polycystin 1, in particular in loop 3. It is likely that the differences in disease phenotype and severity between $Pkd1^{L/L}$ and $Pkd1^{\Delta 34/\Delta 34}$ mice may be related to the level of expression and/or nature of the respective mutant protein. Both mutant proteins are transcribed, as judged by Northern blots or PCR analysis. It has not yet been determined whether the *pkd1Δ34* allele encodes a stable protein. The present data indicate that the protein encoded by L3946* is expressed in homozygous mutants, in the same tissues, and in a pattern that is indistinguishable histologically from that of the WT protein. We speculate that the expressed L3946* polycystin 1 disrupts the normal maturation and/or structural integrity of mature vessels and ductal epithelia in homozygous embryos. Haplo insufficiency in this case is compatible with a normal vascular (and epithelial) phenotype at least up to 7 months of age. A recent correspondence finds that heterozygotes at 16 months of age or older eventually do develop renal cysts, (29). Whether our heterozygote animals will display a cystic phenotype at perhaps an earlier age will be examined.

Expression of polycystin 1 in vascular smooth muscle cells and in endothelia has been previously reported (18, 19). Polycystin 1 also has been detected at intercellular junctions in cultured human umbilical vein endothelium (19), and we found that polycystin 1 is coexpressed with the junctional protein ZO1, a member of the MAGUK (membrane-associated guanylate kinase) protein family, in adult rat tubular epithelium (unpublished observations). The expression of polycystin 1 in the above tissues may account for the observed vascular defect in $Pkd1^{L/L}$ mice. Reciprocal cross-talk between endothelium and surrounding mesenchyme is crucial in the normal assembly of a blood vessel structure. Binding of mesenchymally derived angiopoietin-1 to its endothelial cell receptor TIE2 induces the release of the mesenchymal cell chemoattractant platelet-derived growth factor (PDGF) (30). Upon mesenchymal-endothelial cell contact, active transforming growth factor type β (TGF-β) is produced, which down-regulates endothelial cell proliferation and migration (31, 32) and induces the differentiation of mesenchymal cells into vascular smooth muscles (33) and deposition of a basement membrane matrix (34, 35). Continuous local activation of TGF-β also may be important for the structural maintenance of the vasculature (36). Polycystin 1 expressed in endothelium and smooth muscle cells normally may preserve vascular integrity during angiogenesis by stabilizing adhesion of these already differentiated cells to each other or to the extracellular matrix. In favor is the finding that mesenchymal recruitment and differentiation appear normal in $Pkd1^{L/L}$ mice, and the defect in vascular fragility is morphologically distinct and occurs at a later stage compared with that reported in TIE2-, PDGF-, TGF-β-, or angiopoeitin-1 knockout mice (37–41). Expression of polycystin 1 in subepithelial smooth muscles suggest a similar role of polycystin 1 in morphogenesis and structural stability of some ductal epithelium.

The reported apical junctional location of polycystin 1 in epithelial and endothelial cells also may be causally related to the s.c. edema and cyst formation observed in the $Pkd1^{L/L}$ mutant mice. Findings favoring this alternative (although not necessarily mutual) explanation is the detection of fluorescent dextran in the junctional regions of endothelia (Fig. 3*F*), and the occasional presence of nucleated red cells migrating across endothelial junctions in mutant (but not normal) embryos (Fig. 3*B*). It may be relevant that in the $Pkd1^{L/L}$ embryos and those described by Lu *et al.* (21) cyst formation first is observed in the proximal nephron, where tight junctions possess only one junctional strand (42). Recent work has elucidated crucial roles for intercellular junctions in cell growth, differentiation, polarity, and survival, processes that are abnormal in ADPKD (43). Interference with the formation of intercellular junctions induces the loss of cell polarity and growth regulation in *Drosophila* embryos homozygous for null mutants of the *dlg* gene, a tumor suppressor homologue of the junctional membrane-associated guanylate kinase (MAGUK) family member

ZO1 (44). Also, vulval cells from *Caenorhabditis elegans* with mutation in LIN2, an invertebrate MAGUK family member, are not properly polarized and do not differentiate (45). The normal electron microscopy appearance of tight junctions in the *Pkd1*$^{L/L}$ embryos does not exclude a functional abnormality *in vivo*, because significant changes in permeability have been observed despite normally appearing cell–cell junctions (46, 47). Intercellular junctions are enriched in several classes of signaling proteins, including nonreceptor tyrosine kinases, protein kinase C, β catenin, small G proteins, and heterotrimeric G proteins, and recent data suggesting an interaction of polycystin 1 with heterotrimeric G proteins and the Wnt pathway have been published (48, 49).

Note Added in Proof. Focal hemorrhage has now been reported in mice homozygous for a *Pkd2* null allele (50).

We thank Dr. Mike Carroll for providing the pPNT plasmid, Dr. En Li for advice and assistance with blastocyst injections, and Drs. Mark Fishman and Scott Baldwin for helpful discussions. This work was supported by a PO1 Grant DK54711 from the National Institutes of Health. K.K. was supported by a fellowship award from the National Kidney Foundation.

1. Dalgaard, O. Z. (1957) *Acta Med. Scand.* **328,** Suppl., 1–255.
2. Grantham, J. J. (1993) *Adv. Intern. Med.* **38,** 409–420.
3. Baert, L. (1978) *Kidney Int.* **13,** 519–525.
4. Gabow, P. A. (1993) *N. Eng. J. Med.* **329,** 332–342.
5. Huston, J. D., Torres, V. E., Sulivan, P. P., Offord, K. P. & Wiebers, D. O. (1993) *J. Am. Soc. Nephrol.* **3,** 1871–1877.
6. Ruggieri, P. M., Poulos, N., Masaryk, T. J., Ross, J. S., Obuchowski, N. A., Awad, I. A., Braun, W. E., Nally, J., Lewin, J. S. & Modic, M. T. (1994) *Radiology* **191,** 33–39.
7. Schievink, W. I., Torres, V. E., Piepgras, D. G. & Wiebers, D. O. (1992) *J. Am. Soc. Nephrol.* **3,** 88–95.
8. Zeier, M., Fehrenbach, P., Geberth, S., Mohring, K., Waldherr, R. & Ritz, E. (1992) *Kidney Int.* **42,** 1259–1265.
9. European Polycystic Kidney Disease Consortium (1994) *Cell* **77,** 881–894.
10. International Polycystic Kidney Disease Consortium (1995) *Cell* **81,** 289–298.
11. Mochizuki, T., Wu, G., Hayashi, T., Xenophontos, S. L., Veldhuisen, B., Saris, J. J., Reynolds, D. M., Cai, Y., Gabow, P. A., Pierides, A., *et al*. (1996) *Science* **272,** 1339–1342.
12. Qian, F., Germino, F. J., Cai, Y., Zhang, X., Somlo, S. & Germino, G. G. (1997) *Nat. Genet.* **16,** 179–183.
13. Daoust, M. C., Reynolds, D. M., Bichet, D. G. & Somlo, S. (1995) *Genomics* **25,** 733–736.
14. Geng, L., Segal, Y., Peissel, B., Deng, N., Pei, Y., Carone, F., Rennke, H. G., Glucksmann-Kuis, A. M., Schneider, M. C., Ericsson, M., *et al*. (1996) *J. Clin. Invest.* **98,** 2674–2682.
15. Griffin, M. D., Torres, V. E., Grande, J. P. & Kumar, R. (1996) *Proc. Assoc. Am. Physicians* **3,** 185–197.
16. Palsson, R., Sharma, C., Kim, K., McLaughlin, M., Brown, D. & Arnaout, M. (1996) *Mol. Med.* **2,** 702–711.
17. Cai, Y., Maeda, Y., Cedzich, A., Torres, V. E., Wu, G., Hayashi, T., Mochizuki, T., Park, J. H., Witzgall, R. & Somlo, S. (1999) *J. Biol. Chem.* **274,** 28557–28565.
18. Griffin, M. D., Torres, V. E., Grande, J. P. & Kumar, R. (1997) *J. Am. Soc. Nephrol.* **8,** 616–626.
19. Ibraghimov-Beskrovnaya, O., Dackowski, W. R., Foggensteiner, L., Coleman, N., Thiru, S., Petry, L. R., Burn, T. C., Connors, T. D., Van Raay, T., Bradley, J., *et al*. (1997) *Proc. Natl. Acad. Sci. USA* **94,** 6397–6402.
20. Peters, D. J., van de Wal, A., Spruit, L., Saris, J. J., Breuning, M. H., Bruijn, J. A. & de Heer, E. (1999) *J. Pathol.* **188,** 439–446.
21. Lu, W., Peissel, B., Babakhanlou, H., Pavlova, A., Geng, L., Fan, X., Larson, C., Brent, G. & Zhou, J. (1997) *Nat. Genet.* **17,** 179–181.
22. Wu, G., D'Agati, V., Cai, Y., Markowitz, G., Park, J. H., Reynolds, D. M., Maeda, Y., Le, T. C., Hou, H., Jr., Kucherlapati, R., *et al*. (1998) *Cell* **93,** 177–188.
23. Li, E., Bestor, T. H. & Jaenisch, R. (1992) *Cell* **69,** 915–926.
24. Zijlstra, M., Li, E., Sajjadi, F., Subramani, S. & Jaenisch, R. (1989) *Nature (London)* **342,** 435–438.
25. Coffin, J. D. & Poole, T. J. (1988) *Development (Cambridge, U.K.)* **102,** 735–748.
26. Stewart, P. A. & Wiley, M. J. (1981) *Dev. Biol.* **84,** 183–192.
27. Grubb, B. R. & Boucher, R. C. (1999) *Phys. Rev.* **79,** 193–214.
28. Pelletier, J., Bruening, W., Kashtan, C. E., Mauer, S. M., Manivel, J. C., Striegel, J. E., Houghton, D. C., Junien, C., Habib, R., Fouser, L., *et al*. (1991) *Cell* **67,** 437–447.
29. Lu, W., Fan, X., Basora, N., Babakhanlou, H., Law, T., Rifai, N., Harris, P. C., Perez-Atayde, A. R., Rennke, H. G. & Zhou, J. (1999) *Nat. Genet.* **21,** 160–161.
30. Folkman, J. & D'Amore, P. A. (1996) *Cell* **87,** 1153–1155.
31. Orlidge, A. & D'Amore, P. A. (1987) *J. Cell. Biol.* **105,** 1455–1462.
32. Sato, Y. & Rifkin, D. B. (1989) *J. Cell. Biol.* **109,** 309–315.
33. Hirschi, K. K., Rohovsky, S. A. & D'Amore, P. A. (1998) *J. Cell. Biol.* **141,** 805–814.
34. Crocker, D. J., Murad, T. M. & Geer, J. C. (1970) *Exp. Mol. Pathol.* **13,** 51–65.
35. Madri, J. A., Pratt, B. M. & Tucker, A. M. (1988) *J. Cell. Biol.* **106,** 1375–1384.
36. Chamley-Campbell, J. H., Campbell, G. R. & Ross, R. (1981) *J. Cell. Biol.* **89,** 379–383.
37. Dickson, M. C., Martin, J. S., Cousins, F. M., Kulkarni, A. B., Karlsson, S. & Akhurst, R. J. (1995) *Development (Cambridge, U.K.)* **121,** 1845–1854.
38. Leveen, P., Pekny, M., Gebre-Medhin, S., Swolin, B., Larsson, E. & Betsholtz, C. (1994) *Genes Dev.* **8,** 1875–1887.
39. Suri, C., Jones, P. F., Patan, S., Bartunkova, S., Maisonpierre, P. C., Davis, S., Sato, T. N. & Yancopoulos, G. D. (1996) *Cell* **87,** 1171–1180.
40. Soriano, P. (1994) *Genes Dev.* **8,** 1888–1896.
41. Vikkula, M., Boon, L. M., Carraway, K. L., 3rd, Calvert, J. T., Diamonti, A. J., Goumnerov, B., Pasyk, K. A., Marchuk, D. A., Warman, M. L., Cantley, L. C., *et al*. (1996) *Cell* **87,** 1181–1190.
42. Brown, D. & Orci, L. (1988) *J. Electron Microsc. Technol.* **9,** 145–170.
43. Wilson, P. (1997) *Am. J. Physiol.* **272,** F434–F442.
44. Woods, D. F. & Bryant, P. J. (1991) *Cell* **66,** 451–464.
45. Hoskins, R., Hajnal, A. F., Harp, S. A. & Kim, S. K. (1996) *Development (Cambridge, U.K.)* **122,** 97–111.
46. Wong, V. & Gumbiner, B. M. (1997) *J. Cell. Biol.* **136,** 399–409.
47. Papini, E., Satin, B., Norais, N., de Bernard, M., Telford, J. L., Rappuoli, R. & Montecucco, C. (1998) *J. Clin. Invest.* **102,** 813–820.
48. Parnell, S. C., Magenheimer, B. S., Maser, R. L., Rankin, C. A., Smine, A., Okamoto, T. & Calvet, J. P. (1998) *Biochem. Biophys. Res. Commun.* **251,** 625–631.
49. Kim, E., Arnould, T., Sellin, L. K., Benzing, T., Fan, M. J., Gruning, W., Sokol, S. Y., Drummond, I. & Walz, G. (1999) *J. Biol. Chem.* **274,** 4947–4953.
50. Wu, G., Markowitz, G. S., Li, L., D'Agati, V. D., Factor, S. M., Geng, L., Tibara, S., Tuchman, J., Cai, Y., Hoon Park, J., *et al.* (2000) *Nat. Genet.* **24,** 75–78.